Proc. of the International Conference on Mechanochemistry and Mechanical Alloying, Kraków, Poland, June 22–26, 2014

Use of Mechanical Alloying for Production of Aluminium Matrix Composites with Non-Agglomerated Nanodiamond Reinforcing Particles

V.A. Popov[a], A.S. Prosviryakov[a], T.B. Sagalova[a], D.M. Többens[b], and Ph.V. Kiryukhantsev-Korneev[a]

[a]National University of Science and Technology "MISIS", Leninsky prospect, 4, 119049 Moscow, Russia

[b]Helmholtz-Zentrum Berlin for Materials and Energy, Albert-Einstein-Str. 15, 12489 Berlin, Germany

Agglomeration is the main problem that prevents large-scale implementation of nanodiamonds in the production of composites. Mechanical alloying was applied for crushing the agglomerates and to obtain uniform distribution of the primary nanodiamond particles in aluminium matrix composites. The commonly used X-ray diffraction method fails to detect non-agglomerated diamond nanoparticles 5 to 6 nm in size, if they are incorporated in a metal matrix. Synchrotron radiation was used for the identification of non-agglomerated nanodiamonds. Scanning electron microscopy and synchrotron investigation showed that mechanical alloying does not lead to transformation of the diamond structure into other allotropic forms of carbon and the nanodiamond reinforcing particles are uniformly distributed in the aluminium matrix.

DOI: 10.12693/APhysPolA.126.1008

PACS: 81.05.Ni, 81.20.Ev

1. Introduction

Aluminium is one of the metals widely used in engineering. There is always an industrial demand for new aluminium based materials with enhanced service properties. One of the ways to enhance service properties is the development of composite materials, including aluminium matrix composites with powdery reinforcing particles [1–5]. Combinations of aluminium with various ceramic and carbon particles are well known composites. The most available particles about 10–100 μm in size are widely used. In this case, there is a limitation on size of the items including the coating, as the non-uniformity of the properties is manifested in the small sized items. Composites with large reinforcements cannot be used in cases when there are strict requirements to the surface quality. These negative effects can be avoided by using nanopowders as reinforcing particles. The nanodiamonds produced by detonation synthesis belong to actual and industrially produced nanopowders [6–8]. The size of the primary nanodiamond particles is 4–6 nm. The problem that hinders wide industrial application of nanodiamonds is agglomeration. If the primary particle size is 5 nm, the agglomerate size is hundreds of micrometers. In this work, mechanical alloying is proposed for breaking the agglomerates [9–13].

2. Materials, methods and equipment

Commercially available aluminium powder (Al-99.99% by weight) with separate particles 20–100 μm and nanodiamonds produced by "Elektrokhimpribor" were used in this research. The size of the primary nanodiamond particles is 4–6 nm, while the agglomerate size is up to 50 μm. The diamond phase content is 95–97%, and the rest is carbon in non-diamond form. The composites with nanodiamond content equal to 5, 10, 25 and 35 vol.% were investigated.

Mechanical alloying was performed in the Retsch PM400 planetary mill under argon atmosphere without surface active materials. The steel jars volume was 500 ml, and steel balls with size of 15 mm in diameter were used as a technological tool. The total powder mass for one steel jar was 60 g with ball-to-powder weight ratio 10:1. Rotation speed was 300 rpm. Mechanical alloying was performed for each composite makeup for 1, 4, and 8 h.

XRD was performed on a Bruker D8 ADVANCE diffractometer using monochromatized Cu K_α radiation (with diffracted-beam monochromator). The morphology and structure of composite granules were investigated with a field emission scanning electron microscope JEOL JSM-6700F. The identification of non-agglomerated nanodiamonds was carried out at the synchrotron BESSY II (Berlin-Adlershof); research was performed on the KMC-2 beamline with a wavelength of 1.5406 Å (8048 eV), equal to Cu K_α radiation [14]. At this wavelength KMC-2 yields 10^8 phot./mm^2/s, so that counting statistics enough for successful observation of nanodiamond peaks are expected.

The element composition was measured with the help of glow discharge-optical emission spectroscopy by the apparatus Profiler 2 (Horiba Jobin Yvon, France) on specially prepared samples. The analysis area was 4 mm in diameter. The discharge power was 35 W, argon pressure — 700 Pa, blowing time of the disruptive distance by argon — 30 s. The measurement was controlled and data were processed using the Quantum-XP software. During

the measurement the dependence of the signal's intensity on the etching time was recorded, and then based on those dependences the dependence of elements concentrations on depth with the use of calibrations were calculated [15].

3. Results and discussion

Processing in the planetary mill for 1 h is not enough for complete breakdown of agglomerates and uniform distribution of nanodiamonds in the matrix for all the ND concentrations. Eight hours of processing for the ND concentrations over 25 vol.% results in the formation of aluminium carbide (Fig. 1), that makes using this material impossible. Mechanical alloying of aluminium powders with nanodiamonds for 4 h for all the ND concentrations enabled obtaining composite granules with uniform distribution of non-agglomerated nanodiamond particles in the aluminium matrix. There was no contamination.

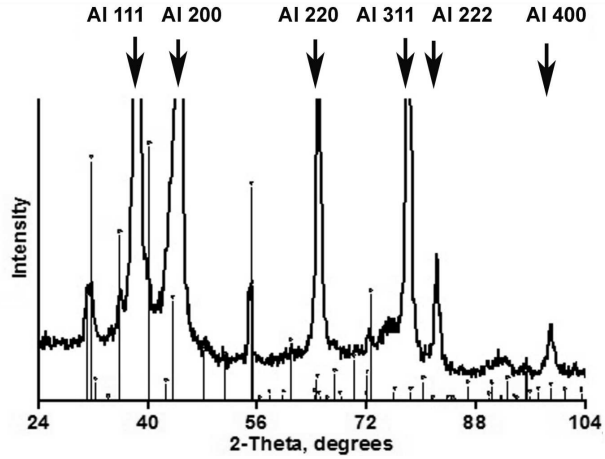

Fig. 1. X-ray diffraction patterns from mixture "Al + 35%(vol)ND" after 8 h treatment in planetary mill: arrows show aluminium peaks; lines show aluminium carbide peaks.

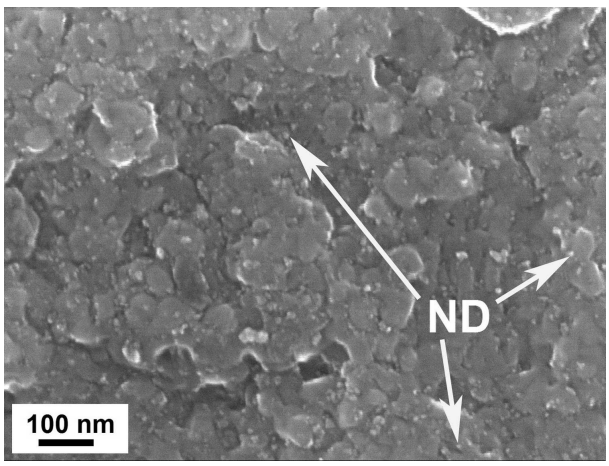

Fig. 2. Non-agglomerated nanodiamonds on the granule surface of the composite "Al + 10%(vol)ND".

Figure 2 shows the surface morphology of such composite granules, where it is evident that the agglomerates are fully broken down and the reinforcing particles are non-agglomerated and are separated from one another.

Determination of the carbon content on the samples with a 10 vol.% nanodiamond content showed that the carbon content corresponds to the nanodiamond content in the original condition. Figure 3 shows the elements distribution profile by the sample depth, starting from 1μm and deeper (the data obtained to the depth of 1μm were not considered because of the discharge stabilization). According to the data obtained, the concentration of carbon in the sample was 9–10% in conversion to volume percent. Average by depth oxygen concentration did not exceed 2%.

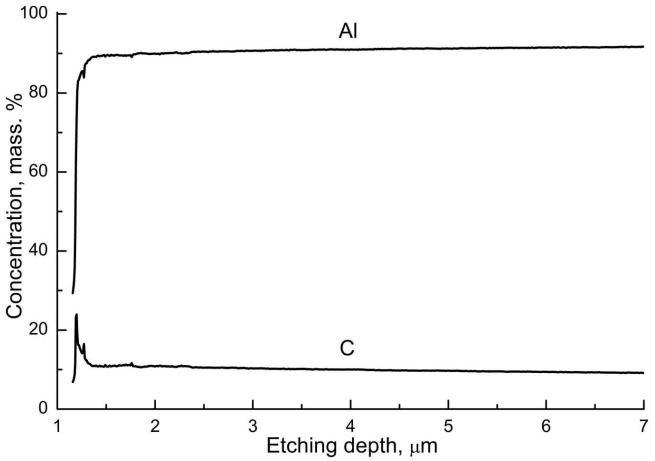

Fig. 3. Aluminium and carbon distribution profile by the sample depth.

To make sure that there was no transformation of the diamond structure into other allotropic carbon forms during treatment in the planetary mill, it was required to identify the nanodiamonds. Figure 4 shows X-ray diffraction patterns from the initial powder mixture (agglomerate size of nanodiamonds is 10–50 μm) and from the composite granules where nanodiamonds are non-agglomerated (the size of the primary nanodiamond particles is 4–6 nm). This figure shows that the intensity of the X-ray radiation on traditional X-ray phase analysis installations was not enough for the case of even distribution of non-agglomerated nanodiamonds in the metal matrix.

To identify non-agglomerated nanodiamonds in the metal matrix, it was proposed to employ synchrotron radiation [16, 17]. In advance X-ray diffraction patterns from the primary nanodiamond powder with the employment of synchrotron radiation were obtained. The size of the coherently scattering domains calculated by the Scherrer equation was 3 nm. It can be explained by the fact that not all the nanodiamond particles are a single crystal. Quite often there are twin crystals and in this case the coherently scattering domain may be reduced to

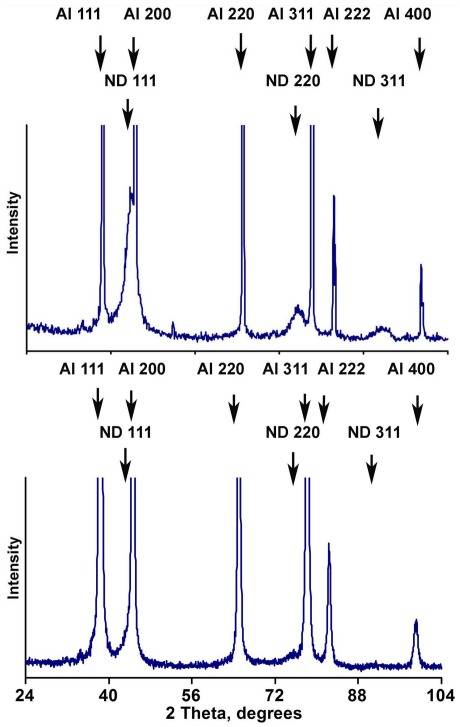

Fig. 4. X-ray diffraction patterns from mixture of initial powders (top) and composite granules after mechanical alloying during 4 h (bottom) of combination "Al + 10%(vol)ND".

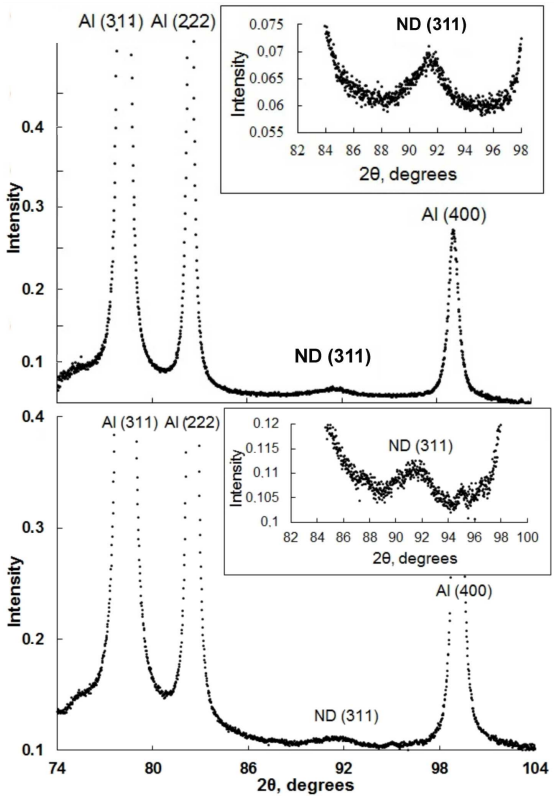

Fig. 5. X-ray diffraction patterns from aluminium composites with 10%(vol) (top) and 5%(vol) (bottom) of nanodiamonds with the employment of synchrotron radiation.

less than 1 nm. Figure 4 (top) shows that diamond peak (311) is separated from the aluminium peaks; that is why to identify the nanodiamonds in the aluminium matrix exactly this peak was selected. X-ray diffraction patterns from aluminium composites with 10 and 5 vol.% of nanodiamonds with the employment of synchrotron radiation were obtained (Fig. 5). It is evident that these methods make it possible to identify nanodiamonds as the position of the peak obtained strictly coresponds to the position of the diamond peak and its width compares well with the one calculated by the Scherrer equation based on the condition that the coherently scattering domain have a diameter of 3 nm. Distinction between broadening resulting from domain size or microstrain is foremost from the different angular dependence, expressed by the Scherrer formula in the former or the Wilson formula in the later case. Much weaker is the empirically based assumption that size effects primarily result in Lorentzian broadening, while microstrain leads to Gaussian broadening. Refinements of the peak shape of pure nanodiamonds using these models implemented in the TCH pseudo-Voigt profile function [18] showed only Lorentzian broadening with size-like angular dependence. Contributions from the other three possibilities were found to be insignificant. For the threatened nanodiamonds in metal matrix, only one diffraction peak is experimentally accessible, which makes it impossible to test the angular dependence of the broadening. However, in all samples only Lorentzian broadening was observed. It is thus justified to interpret the broadening in all cases in terms of domain size.

4. Conclusion

There was developed a method of producing composite material with aluminium matrix reinforced by non-agglomerated nanodiamond particles. It is proved that mechanical alloying allows obtaining complete disintegration of initial nanodiamond agglomerates and uniform distribution of diamond nanoparticles in aluminium matrix. But eight hours (and more) of processing by mechanical alloying results in the formation of aluminium carbide.

Application of synchrotron radiation allows identifying non-agglomerated nanodiamond particles in aluminium matrix. The developed method for obtaining the composite material does not result in the transformation of the nanodiamonds into other allotropic forms of carbon.

Acknowledgments

The research leading to these results has received funding from the European Union's Seventh Framework Programme (FP7/2007-2013) under the EFEVE project, grant agreement 314582; the Russian Foundation for Basic Research (Project No. 12-08-00210), and the Helmholtz-Zentrum Berlin for Materials and Energy (BESSY II, proposal 120812).

References

[1] S. Kasman, S. Ozan, L. Feray Guleryuz, R. Ipek, *Acta Phys. Pol. A* **123**, 221 (2013).

[2] S. Kasman, L. Feray Guleryuz, S. Ozan, R. Ipek, *Acta Phys. Pol. A* **123**, 224 (2013).

[3] C.R. Bradbury, J-K. Gomon, L. Kollo, H. Kwon, M. Leparoux *J. Alloys Comp.* **585**, 362 (2014).

[4] P. Fuchs, H. Hagendorfer, Y.E. Romanyuk, A.N. Tiwari, *Phys. Status Solidi A*, article first published online: 4 July 2014.

[5] D. Nunes, M. Vilarigues, J.B. Correia, P.A. Carvalho, *Acta Mater.* **60**, 737 (2012).

[6] P.Ya. Detkov, V.A. Popov, V.G. Kulichikhin, S.I. Chukhaeva, in: *Molecular Building Blocks for Nanotechnology: From Diamondoids to Nanoscale Materials and Applications*, Topics in Applied Physics, Vol. 109, Eds. G.A. Mansoori, T.F. George, G.P. Zhang, L. Assoufid, Springer, New York 2007, p. 29.

[7] S. Turner, O. Shenderova, F. Da Pieve, Y. Lu, E. Yücelen, J. Verbeeck, D. Lamoen, G. Van Tendeloo, *Phys. Status Solidi A* **210**, 1976 (2013).

[8] V.A. Popov, in: *Nanocomposites: Synthesis, Characterization and Applications*, Ed. X.Y. Wang, Nova Science Publ., New York 2013, p. 369.

[9] C. Suryanarayana, N. Al-Aqeeli, *Prog. Mater. Sci.* **58**, 383 (2013).

[10] H. Gencer, N.E. Cengiz, V.S. Kolat, T. Izgi, S. Atalay, *Acta Phys. Pol. A* **125**, 214 (2014).

[11] S. Scudino, M. Sakaliyska, M. Stoica, K.B. Surreddi, F. Ali, G. Vaughan, A.R. Yavari, J. Eckert, *Phys. Status Solidi (RRL)* **2**, 272 (2008).

[12] D. Nunes, V. Livramento, U.V. Mardolcar, J.B. Correia, P.A. Carvalho, *J. Nucl. Mater.* **426**, 115 (2012).

[13] B. Ertuğ, B.N. Çetiner, G. Sadullahoğlu, H. Gökçe, Z.E. Erkmen, M.L. Öveçoğlu, *Acta Phys. Pol. A* **123**, 188 (2013).

[14] A. Erko, I. Packe, C. Hellwig, in: *AIP Conf. Proc.: Synchrotron Radiation Instrumentation*, Eds. P. Pianetta, J. Arthru, S. Brennan, Vol. 521, American Institute of Physics, 2000, p. 415.

[15] Ph.V. Kiryukhantsev-Korneev. *Protect. Met. Phys. Chem. Surf.* **48**, 585 (2012).

[16] H. Wiedemann, *Synchrotron Radiation, Advanced Texts in Physics*, Vol. XIII, Springer, Berlin 2003.

[17] T. Tangcharoen, W. Klysubun, C. Kongmark, W. Pecharapa, *Phys. Status Solidi A*, article first published online, 2014.

[18] P. Thompson, D.E. Cox, J.B. Hastings. *J. Appl. Crystallogr.* **20**, 79 (1987).